Sedimentary Geology 339 (2016) 104–114

Contents lists available at ScienceDirect

Sedimentary Geology

journal homepage: www.elsevier.com/locate/sedgeo

Micropaleontology of the 2013 Typhoon Haiyan overwash sediments from the Leyte Gulf, Philippines

Jessica E. Pilarczyk [a,b,c,*], Benjamin P. Horton [b,c,d,e], Janneli Lea A. Soria [c,e], Adam D. Switzer [c,e], Fernando Siringan [f], Hermann M. Fritz [g], Nicole S. Khan [b,d], Sorvigenaleon Ildefonso [c], Angelique A. Doctor [f], Mikko L. Garcia [f]

[a] Department of Marine Science, University of Southern Mississippi, Stennis Space Center, MS 39529 USA
[b] Sea Level Research, Department of Marine and Coastal Science, Rutgers University, New Brunswick, NJ 08901 USA
[c] Earth Observatory of Singapore, Nanyang Technological University, Singapore
[d] Institute of Earth, Ocean, & Atmospheric Sciences, Rutgers University, New Brunswick, NJ 08901 USA
[e] Asian School of the Environment, Nanyang Technological University, Singapore
[f] Marine Science Institute, University of the Philippines, Diliman, Quezon City, Philippines
[g] School of Civil and Environmental Engineering, Georgia Institute of Technology, Atlanta, GA 30332 USA

ARTICLE INFO

Article history:
Received 17 December 2015
Received in revised form 1 April 2016
Accepted 2 April 2016
Available online 12 April 2016

Editor: Dr. J. Knight

Keywords:
Tropical cyclone
Overwash
Foraminifera
Testate amoebae
Sediments
Paleotempestology

ABSTRACT

Coastal geologic records allow for the assessment of long-term patterns of tropical cyclone variability. However, the accuracy of geologic reconstructions of tropical cyclones is limited by the lack of modern analogues. We describe the microfossil (foraminifera and testate amoebae) assemblages contained within overwash sediments deposited by Typhoon Haiyan when it made landfall on the islands of Leyte and Samar in the Philippines on 7 November 2013 as a Category 5 super typhoon. The overwash sediments were transported up to 1.7 km inland at four study sites. The sediments consisted of light brown medium sand in a layer <1 to 8 cm thick. We used Partitioning Around a Medoid (PAM) cluster analysis to identify lateral and vertical changes in the foraminiferal and testate amoebae data. The presence of intertidal and subtidal benthic, and planktic foraminifera that were variably unaltered and abraded identify the microfossil signature of the overwash sediments. Agglutinated mangrove foraminifera and testate amoebae were present within the overwash sediments at many locations and indicate terrestrial scouring by Haiyan's storm surge. PAM cluster analysis subdivided the Haiyan microfossil dataset into two assemblages based on depositional environment: (1) a low-energy mixed-carbonate tidal flat located on Samar Island (Basey transect); and (2) a higher-energy clastic coastline near Tanauan on Leyte Island (Santa Cruz, Solano, and Magay transects). The assemblages and the taphonomy suggest a mixed provenance, including intertidal and subtidal sources, as well as a contribution of sediment sourced from deeper water and terrestrial environments.

1. Introduction

Landfalling tropical cyclones pose a hazard to the concentrations of population, economic production, and static infrastructure along the coastlines of the Philippines. The Philippines are in close proximity to the Main Development Region (MDR) in the North Pacific (Pun et al., 2013), which is the most active tropical cyclone region in the world (Lin et al., 2013). Numerous tropical cyclones have made landfall on the Philippines (e.g., Typhoon Agnes in 1984, Typhoon Mike in 1990, Typhoon Thelma in 1991, and Typhoon Hagupit in 2014; e.g., Garcia-Herrera et al., 2007; Ribera et al., 2008; NDRRMC, 2014), including Typhoon Haiyan, which was one of the most intense storms on record. Despite the history of typhoon activity in the Philippines, we lack an understanding of the role of recent warming on tropical cyclone activity because of the length of the instrumental record (Landsea et al., 2006). Fortunately, proxy records of overwash sediments are transforming our ability to detect and analyze the underlying climatic forcing for tropical cyclone activity over the last several millennia (Lane et al., 2011; Brandon et al., 2013; Denommee et al., 2014; Donnelly et al., 2015).

Storm surges associated with past tropical cyclones deposit overwash sediments that become preserved in the geologic record. The identification of overwash sediments is commonly based on the recognition of anomalous sand layers in otherwise low-energy coastal settings (e.g., Liu and Fearn, 1993, 2000; Donnelly et al., 2001) supported by microfossils, which can indicate provenance of sediment (e.g., Collins et al., 1999; Hippensteel and Martin, 1999; Scott et al., 2003; Hippensteel et al., 2005; Hawkes and Horton, 2012). Marine microfossils, such as foraminifera, are often present in overwash sediments due to the landward transport and deposition of coastal and marine sediment during a

* Corresponding author.

http://dx.doi.org/10.1016/j.sedgeo.2016.04.001
0037-0738/

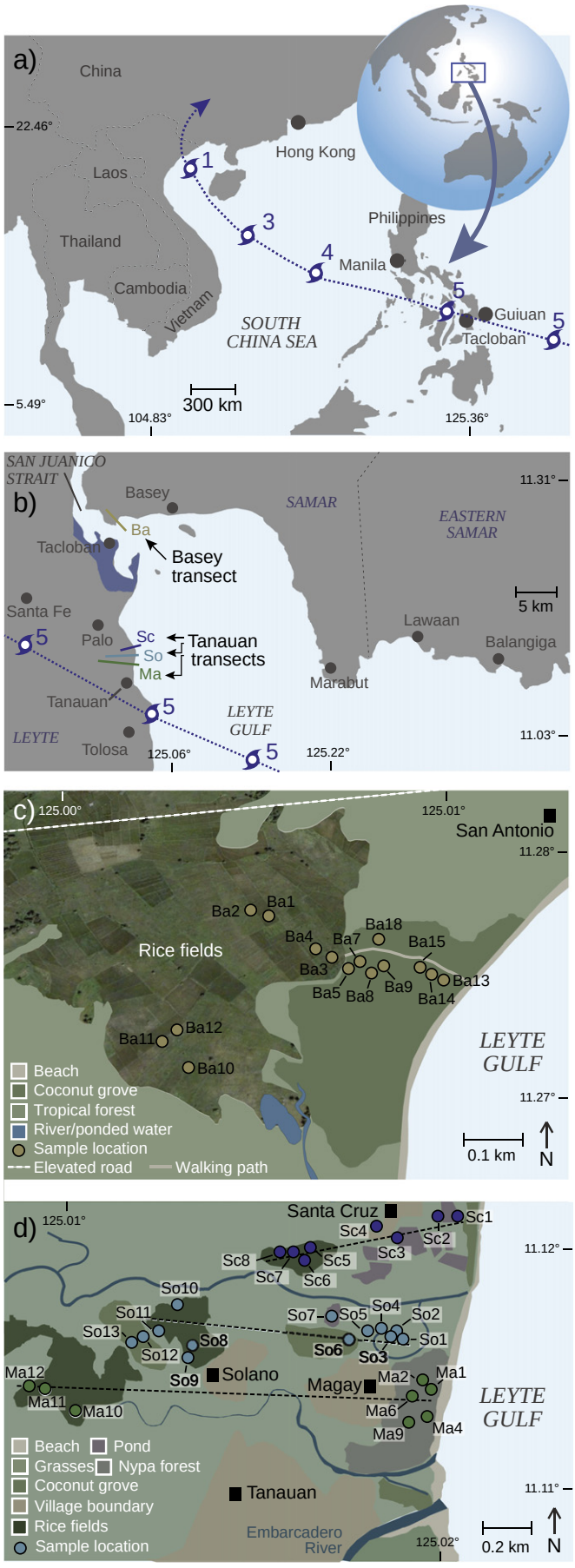

tropical cyclone's storm surge (e.g., Hippensteel and Martin, 1999; Scott et al., 2003; Lane et al., 2011). Testate amoebae are commonly found in freshwater environments (e.g., Ogden and Hedley, 1980; Charman, 2001; Smith et al., 2008) and have potential as indicators of terrestrial scouring by a storm surge.

An obstacle in identifying past tropical cyclones in the geologic record is the lack of a modern analogue. However, the microfossil signature of modern tropical cyclone overwash sediments can provide insight into their long-term preservation in the fossil record (Otvos, 1999; Scott et al., 2003; Hippensteel et al., 2005), and can be directly compared to similar studies of overwash sediments deposited by tsunamis (Dominey-Howes et al., 2000; Hawkes et al., 2007; Clark et al., 2011; Goff et al., 2011; Pilarczyk et al., 2012). The majority of studies that employ foraminifera to document tropical cyclone sediments have been conducted in temperate environments from the Atlantic Ocean (Scott et al., 2003; Kortekaas and Dawson, 2007; Hippensteel et al., 2013) and Gulf of Mexico (Williams, 2009; Hawkes and Horton, 2012; Rabien et al., 2015), with little research in tropical or semi-tropical environments (Strotz and Mamo, 2009; Pilarczyk and Reinhardt, 2012) such as the Philippines.

In this paper we document the microfossil assemblages of the Typhoon Haiyan overwash sediments, collected less than two months after the storm made landfall on 7 November 2013. A series of trenches and cores was obtained at four sites from two contrasting environments (one mixed-carbonate site and three clastic sites) along the northwestern Leyte Gulf coastline (Fig. 1). Haiyan sediments were discriminated from underlying pre-storm sediments by the presence of intertidal and subtidal benthic, and planktic foraminifera. The unaltered (i.e., pristine) and abraded nature of the foraminifera within the Haiyan overwash sediments point to a mixed provenance, including terrestrial, intertidal, subtidal, and deeper sources. Evidence of terrestrial scour by the storm surge is indicated by the presence of agglutinated mangrove foraminifera and freshwater testate amoebae. The microfossil signature of the overwash sediments deposited by Typhoon Haiyan serves as the only modern analogue of a landfalling typhoon in the Philippines, and may be important to the recognition and interpretation of older storm sediments preserved in coastal sequences at this location, as well as other tropical settings worldwide.

2. Typhoon Haiyan

Typhoon Haiyan (locally known as Yolanda) was the thirtieth named storm in the 2013 Pacific typhoon season. Haiyan began as a westward-tracking low-pressure system on 2 November that developed into a tropical storm by 0000 UTC on 4 November and rapidly intensified to typhoon intensity eight hours later (Joint Typhoon Warning Center, 2014; Fig. 1a). By 7 November, the Joint Typhoon Warning Centre (JTWC) reported gusts of up to 314 km/h three hours before initial landfall and declared the storm a Category 5, designating Typhoon Haiyan as one of the most intense tropical cyclones. At 2040 UTC on 7 November, Haiyan made its first landfall over Guiuan, Eastern Samar and continued west-northwest across the Leyte Gulf where it made its second landfall over Tolosa and the Greater Tacloban area at 2300 UTC (Fig. 1b). Following six landfalls in the Philippines (Guiuan and Tacloban in Leyte; Daanbantayan and Bantayan in Cebu; Concepcion in Iloilo; and Busuanga in Palawan), Haiyan weakened to a Category 2 before striking northeastern Vietnam at 0000 UTC on 8 November, after which the storm tracked northeast and dissipated over China (Fig. 1a).

Fig. 1. (a) Location map of the Philippines showing track of Typhoon Haiyan (blue dotted line). Major changes in typhoon intensity are indicated in blue and are expressed as Saffir–Simpson categories. (b) Map of the Leyte Gulf indicating location of Tacloban (blue shaded area), transects Ba–Ma, and Typhoon Haiyan's track (JTWC, 2014). (c,d) Detailed map of Ba (Basey), Sc (Santa Cruz), So (Solano), and Ma (Magay) indicating sample locations and major geomorphological features.

Typhoon Haiyan was associated with severe rainfall (491 mm) and high wind speeds (10 min sustained wind speeds of 230 km/h), but most of the damage was caused by the 5- to 7-m-high storm surge (Mori et al., 2014; Nguyen et al., 2014; Tajima et al., 2014; Soria et al., 2016b). The coastlines of the Leyte Gulf sustained the greatest impact, with destruction centered near Tacloban, which sits less than 5 m above mean sea level (MSL). Storm surge heights (elevation of terrain + flow depth above terrain) and inundation distances (inland extent of marine incursion) from coastlines surrounding the Leyte Gulf (including our four study sites) are presented in Soria et al. (2016b).

3. Site description

The Leyte Gulf, ~580 km southeast of the capital city Manila, is bordered by two islands separated by the narrow San Juanico Strait, Leyte Island to the west, and Samar Island to the north and east (Fig. 1). The seismically active Philippine Fault bisects Leyte Island, which is made up of Pliocene-Quaternary volcano cones and Tertiary volcaniclastic rocks and sediments (Allen, 1962; Duquesnoy et al., 1994). Quaternary alluvium, consisting of unconsolidated, poorly sorted sands (Travaglia et al., 1978; Suerte et al., 2005) characterizes the Leyte Gulf side of Samar Island. Sediment inputs to the northern Leyte Gulf include biogenic sediments in reef areas, littoral sediment transported by waves, terrigenous material transported by high rainfall through rivers (e.g., clastics and volcanic residuals; Hart et al., 2002), and deeper offshore sediment carried landward by storms.

Our study focused on a series of four transects from two islands: Basey (Ba) on Samar Island; and the Tanauan transects (Santa Cruz, Sc; Solano, So; and Magay, Ma) on Leyte Island (Fig. 1c,d). The coastline at Basey is characterized by a low-energy mixed-carbonate tidal flat. A gently sloping, narrow sandy beach is present, but was heavily eroded by Typhoon Haiyan. Coconut groves and rice fields are found landward of the beach. The Tanauan coastline is characterized by a higher-energy, wave dominated system. The coastline is a broad, gently sloping coastal plain that is drained by the Embarcadero River (Fig. 1d) and consists of a mixture of siliciclastic and volcaniclastic sediments. The beach at all three Tanauan transect sites was also heavily eroded by Typhoon Haiyan, with coconut groves, ponds, and rice fields occurring farther landward (Fig. 1d; Supplementary Fig. S1). At Magay, *Nypa fruticans* Wurmb, a species of palm adapted to mangrove environments, is found in waterlogged and densely vegetated patches that are associated with incised intertidal channels.

The transects at Samar and Leyte Islands were located in regions that were impacted by high storm surges (Soria et al., 2016b) and experienced minimal anthropogenic alteration in the weeks following Haiyan's landfall. Three closely spaced transects near Tanauan were chosen to assess variability within the overwash sediments. The transects extend from the shoreline to the landward limit of the Haiyan overwash sediments. We attempted to sample the full coastal gradient from the shoreline to the Haiyan inundation limit, however, storm damage (e.g., flooding, destroyed roads) prevented the survey team from accessing certain areas.

4. Methods

In January 2014, we collected sediments from our four transects (Fig. 1b). A detailed lithostratigraphic investigation was completed along each transect from a series of sampling stations. Samples were collected using a hand gouge corer or by excavating shallow trenches. The location of all sampling stations was determined by handheld GPS. At each station we collected one sediment sample from the midpoint (if available) of the Haiyan sediments and one sample from the underlying sediment. At three stations (spaced 50 m apart) within the *Nypa* forest at Magay (transect Ma), where the Haiyan sediments were exposed at the surface, we dug shallow trenches (Ma4, Ma6, and Ma9; Fig. 1d). The trenches were sampled every 1 cm within the Haiyan sediments and two samples were obtained from the underlying sedimentary layer. Samples were sealed in plastic wrap, and held in refrigerated storage until processing.

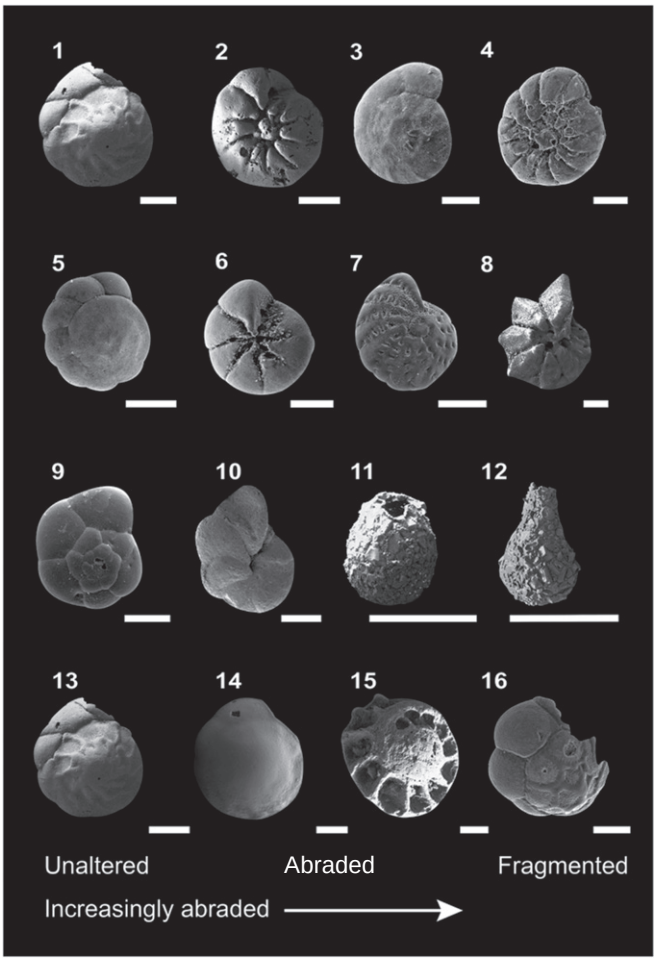

Fig. 2. Scanning electron microscope (SEM) images of dominant taxa and taphonomic characters. All scale bars are equal to 100 μm. (1,2) *Ammonia convexa*, (3,4) *Ammonia parkinsoniana*, (5,6) *Ammonia tepida*, (7) *Elphidium striatopunctatum*, (8) *Pararotalia* sp., (9) *Trochammina inflata*, (10) *Entzia macrescens*, (11) *Centropyxis* spp., and (12) *Difflugia* spp. Taphonomic states of *Ammonia*: unaltered (13), abraded (14,15), and fragmented (16).

At Basey on Samar Island, we collected sediments along a shore normal transect (Ba) consisting of 15 gouge cores (Ba1 to Ba18; Ba 6, 16, and 17 were not sampled) from the beach (0–30 m along the transect), coconut grove (30–210 m) and rice field (210–360 m) environments (Fig. 1c). At the Santa Cruz site, we collected sediments along a shore normal transect (Sc) consisting of 8 gouge cores (Sc1 to Sc8) that extended from the beach (0–10 m), to a low-lying grassy area with ponds (10–530 m), to a rice field (550–890 m). At Solano, sediments were obtained from a shore normal transect (So) that consisted of 13 gouge cores (So1 to So13) from several environments including: an extensive, low-lying grassy area interspersed with shallow ponds (260–1400 m), a rice field (1400–1600 m), and a coconut grove (≥1600 m). At Magay, we collected sediments along a shore normal transect (Ma) consisting of 5 gouge cores (Ma1, Ma2, Ma10–12) and three trench sections (Ma4, Ma6, Ma9) that extended from the shoreline (0–20 m), to a low-lying grassy area (20–120 m), to a fringing *Nypa* forest (120–540 m), to a rice field (1100–1690 m; Fig. 1d). The transect extended through the village of Magay (between 540 m and 1100 m), which consisted of several dozen homes and buildings before the typhoon made landfall.

We conducted microfossil analysis on all core and trench samples. For microfossil analysis, 5 cm^3 sediment samples were washed over a 32 μm sieve to retain foraminifera (intertidal to marine organisms) and testate amoebae (freshwater organisms) tests, and wet split to obtain counts of ~300 specimens. Foraminiferal taxonomy followed Loeblich and Tappan (1987), Debenay (2013), and Hayward et al. (2004), and species identification was confirmed using the Cushman Collection of Foraminifera at the National Museum of Natural History, Smithsonian Institute. We interpreted the foraminiferal data in relation to studies by Glenn-Sullivan and Evans (2001), Hewins and Perry (2006), Lacuna et al. (2013), and Lacuna and Alviro (2014), that examined modern foraminifera from select coastal zones throughout the Philippines. Testate amoebae were identified to the genus level using Ogden and Hedley (1980). Foraminifera (both calcareous and agglutinated species) were divided into small (<250 μm) and large (>250 μm) test sizes by means of sieving. Calcareous species were categorized using the same taphonomic criteria defined by Pilarczyk et al. (2011), which includes unaltered, abraded (including corroded and edge rounded specimens), and fragmented forms (Fig. 2). An individual foraminifera can be both abraded and fragmented. The taphonomic condition of individual foraminifera has previously been used to interpret overwash sediments by assessing depth of scour and origin of sediment (e.g., Goff et al., 2011; Pilarczyk et al., 2012). All microfossil results are listed in Supplementary Tables S1–S4.

We used Partitioning Around a Medoid (PAM) cluster analysis (Kaufman and Rousseeuw, 1990) of the relative abundance of foraminiferal and testate amoebae assemblages and taphonomic characteristics to discriminate the Haiyan overwash sediments from underlying sediment. PAM cluster analysis was also used to identify lateral changes in overwash sediments at Basey and Tanauan. Only categories with a minimum abundance of 5% in at least one sample were used in cluster analysis. Abundances were then used to calculate *z*-scores. *Z*-scores are a means of standardizing datasets by assessing how many standard deviations a value is from the mean. A *z*-score of 0 indicates the value is the same as the mean, whereas a positive or negative score indicates how many standard deviations the value is above (positive score) or below (negative score) the mean. We performed PAM cluster analysis following the methods of Kemp et al. (2012), using the 'cluster' package in R (Maechler et al., 2005). Silhouette plots generated by PAM range in width from -1 to 1 and are an estimate of a sample's classification, where values close to -1 are those that are incorrectly classified, and those close to 1 indicate assignment to an appropriate cluster. We used the maximum average silhouette width to determine the number of clusters within each of our cluster scenarios.

5. Results

5.1. Basey transect (Ba)

The Typhoon Haiyan surge height at Basey was up to 6.5 m above MSL (Soria et al., 2016b). Inundation reached at least 1 km inland, whereas the corresponding overwash sediments were only found up to 360 m. The Haiyan overwash sediments consist of medium to fine sand and, where present, ranged in thickness from 8 cm closest to the shoreline to <1 cm in the rice fields (Supplementary Table S1). The overwash sediments were light brown (10 YR 7/2) in color and carbonate-rich, containing foraminifera and fragments of corals and mollusks that are similar to those found in modern nearshore and beach sediments. The Haiyan sediments overlie either coconut grove or rice field soils with a sharp stratigraphic contact. However, at the time of sampling, post-typhoon vegetation growth in the rice fields (i.e., Supplementary Fig. S1c) had already begun to obscure the contact.

The Haiyan overwash sediments at Basey contain abundant foraminifera. Concentrations of foraminifera are highest at sample sites closest to the shoreline (up to 6320 foraminifera per 5 cm^3), and begin to markedly decrease beginning at ~100 m inland, where concentrations

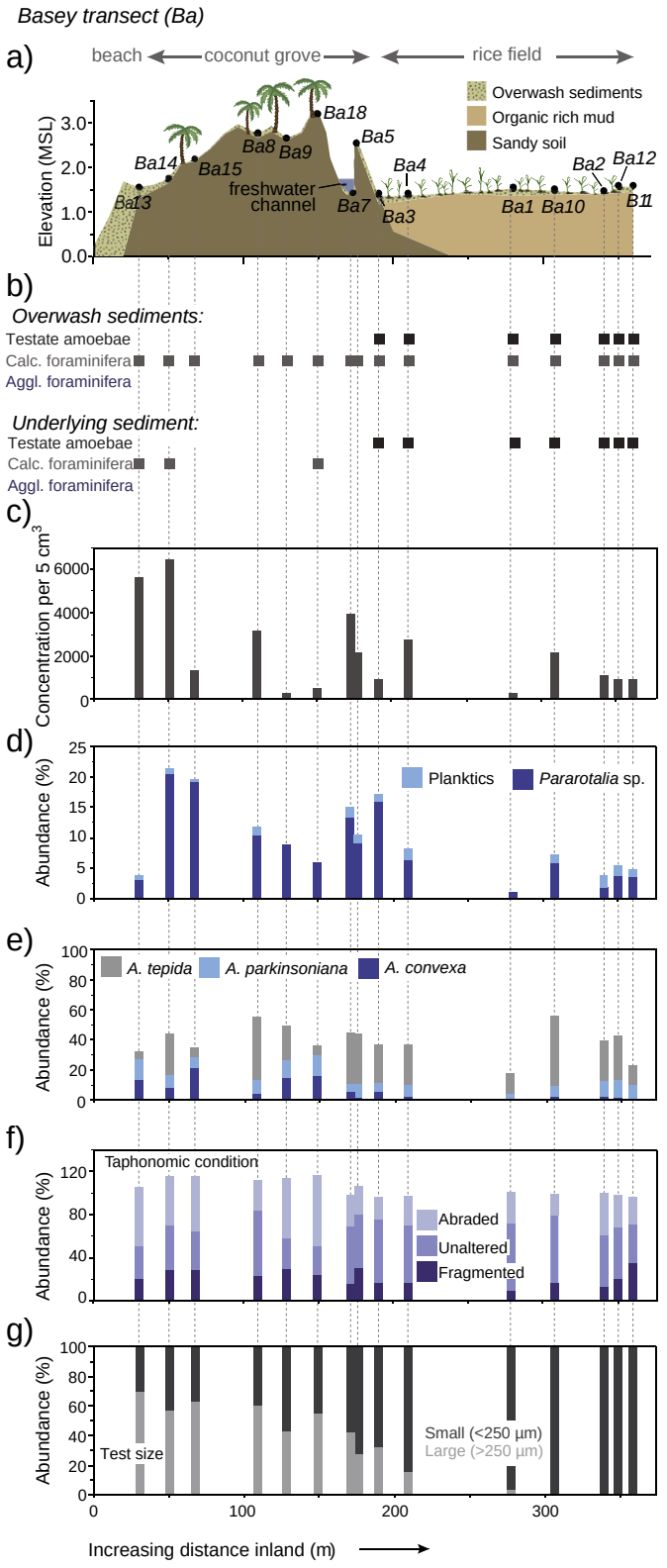

Fig. 3. Changes in the microfossil assemblage with increasing distance inland for Ba (Basey). (a) Elevation profile indicating major geomorphological features, location of sample sites (black circle), and thickness of the overwash sediments. (b) Presence *vs.* absence of testate amoebae and foraminifera (calcareous and agglutinated) for each sample location. (c) Concentration of foraminifera per 5 cm^3. (d,e) Relative abundances of dominant foraminiferal species within the overwash sediments. (f) Taphonomic condition of calcareous foraminifera. An individual foraminifera can be both abraded and fragmented. (g) Abundances of small and large tests within the overwash sediments. Bar graphs are stacked histograms.

decrease to 45 foraminifera per 5 cm^3 (Fig. 3; Supplementary Table S1). The Haiyan assemblage consists exclusively of calcareous species such as *Ammonia tepida* (Cushman, 1926; 4%–47%), *Ammonia convexa* Collins, 1958 (0%–22%), and *Pararotalia* sp. (2%–20%; Fig. 2). Planktic foraminifera are present in the overwash sediments at all sampled locations (<2%) except where total concentration is very low (Ba9, Ba18, and Ba1). Unaltered deeper-dwelling species such as *Eponides repandus* (Fichtel and Moll, 1798; up to 13%) and *Cibicides tabaensis* Perelis and Reiss (1976; 0%–2%) are also present, but in lower abundances. Testate amoebae are absent from the overwash sediments except at sites landward of Ba3 (190 m from the shoreline), where *Difflugia* spp. are present (3%–63%). The taphonomic condition of foraminifera within the Haiyan sediments includes unaltered, abraded, and fragmented forms. Samples within 150 m of the shoreline are generally dominated by abraded individuals (29%–66%; Supplementary Table S1) with a large test (>250 μm) size (43%–71% of tests). Beginning at ~170 m inland (Ba7), unaltered individuals (38%–64%) with a small test (<250 μm) size (59%–100% of tests) generally dominate the assemblage.

Foraminifera were absent from underlying soil units at all sites except Ba13, Ba14, and Ba18 in the coconut grove. The total concentration of foraminifera in these soils was lower than in the overlying Haiyan sediments (e.g., 125 foraminifera per 5 cm^3 in underlying soils *vs.* 6320 foraminifera per 5 cm^3 in Haiyan sediments at Ba14). The taxonomic assemblage of the soil consists of nearshore species including *A. convexa* (18%–26%), *Ammonia parkinsoniana* (d'Orbigny, 1839; 6%–25%), and *Elphidium striatopunctatum* (Fichtel and Moll, 1798; 25%–36%). Testate amoebae (*Difflugia* spp.) are found at Ba3 (inland extent of the coconut grove) and the rice fields (145–1110 per 5 cm^3). Foraminifera within the soil units are dominantly abraded (82%–100%) and small sized (79%–95%).

5.2. Santa Cruz transect (Sc)

The surge height recorded at Santa Cruz on Leyte Island reached 5.1 m above MSL and inundated up to 3 km inland (Soria et al., 2016b), however, we could only trace the corresponding sedimentary deposit up to 890 m. The Haiyan overwash sediments at Santa Cruz were characterized by a patchy, medium to fine sand (Soria et al., 2016a), variable thickness (<1–7 cm; Supplementary Table S2), a light brown color (10 YR 7/2), and the presence of siliciclastic and volcaniclastic sediments. The overwash sediments overlie either grassy soil, pond sediment, or rice field soil with a gradational contact resulting from post-typhoon bioturbation.

Foraminiferal concentrations within the overwash sediments at Santa Cruz are lower than those observed at Basey (e.g., 5–35 individuals per 5 cm^3 at Santa Cruz *vs.* 45–6320 individuals per 5 cm^3 at Basey; Fig. 4a; Supplementary Table S2). Similar to Basey, concentrations of foraminifera are highest at sample sites closest to the shoreline (e.g., 25–35 foraminifera per 5 cm^3 within 20 m of the shoreline), and lowest at the furthest inland sites (5–20 foraminifera per 5 cm^3 from 440–890 m). The Haiyan assemblage at Santa Cruz is dominated by benthic and planktic calcareous foraminifera. *Ammonia convexa* (0%–33%), and *A. parkinsoniana* (0%–31%) are the most dominant benthic species (Fig. 4a). Planktics (9%–24%) are present at all sites except Sc1 located closest to the shoreline. In general, testate amoebae, including *Difflugia* spp. (up to 73%) and *Centropyxis* spp. (up to 30%), are abundant within the overwash sediments (Fig. 2). The taphonomic condition of foraminifera within the overwash sediments includes unaltered (22%–73%), abraded (17%–78%), and fragmented (16%–51%) forms. The concentration of unaltered individuals at Santa Cruz exceeded abraded and fragmented individuals at all locations except Sc1 and Sc5. In contrast to Basey, the abundance of unaltered individuals was unrelated to distance inland. Similarly, there was no observable relationship between test size and distance inland. Larger foraminifera dominate sites Sc1–Sc2 and Sc5–Sc6 (57%–66%), whereas smaller foraminifera dominate sites Sc3–Sc4 and Sc7–Sc8 (57%–68%).

Foraminifera were absent in all underlying soils. However, pond sediment (120 testate amoebae per 5 cm^3), as well as grass (25–75 testate amoebae per 5 cm^3), and rice field (1025–1270 testate amoebae per 5 cm^3) soils contained abundant *in situ* testate amoebae. The soil underlying the grassy area at Sc1 and Sc2, closest to the shoreline, is dominated by *Centropyxis* spp. (54%–75%). At a distance of 440 m inland, the assemblage switches to one that is dominated by *Difflugia* spp. (85%–93%).

5.3. Solano transect (So)

We were unable to measure the Typhoon Haiyan surge height at Solano; however, it would have been similar to the surge heights measured a few hundred meters shoreward at Santa Cruz (5.1 m above MSL) and Magay (5.4 m above MSL). At Solano, the overwash sediments reached a distance of 1.6 km inland, which is less than the 2.8 km inundation distance reported by Soria et al. (2016b). The overwash sediments at Solano consisted of a patchy fine to medium sand (Soria et al., 2016a) with variable thickness (<1–4.5 cm; Supplementary Table S3), a light brown color (10 YR 7/2), and the presence of siliciclastic and volcaniclastic sediments. A sharp contact between the overwash sediments and the underlying soil was observed at all sites except those located within the rice fields where bioturbation by roots had resulted in a gradational contact.

The total concentration of foraminifera within the overwash sediments at Solano is similar to concentrations observed at Santa Cruz (ranging from 10 to 80 individuals per 5 cm^3; Fig. 4b; Supplementary Table S3). Similarly, the species contained within the overwash sediments are similar at both sites, where shallow intertidal to subtidal benthics as well as planktics dominate the assemblage. *Ammonia convexa* (0%–27%) and *A. parkinsoniana* (0%–20%) are generally the most dominant benthic species (Fig. 2; Fig. 4b). Planktics are found throughout the overwash sediments (4%–33%), including at So13 (10%) located at a distance of 1.6 km inland. Testate amoebae are also present within the overwash sediments at Solano (up to 93% of the Haiyan assemblage). The foraminiferal taphonomic assemblage within the overwash sediments switched at 460 m inland from one that is generally dominated by fragmented individuals (e.g., 54% at So5) to one that is dominated by unaltered individuals (e.g., 100% at So13, 1.6 km from the shoreline). At Solano, test size generally decreased with increasing distance inland (e.g., 45% of foraminifera were small at So1 compared to 82% at So12). Small foraminifera were more abundant in the overwash sediments than larger ones except at So1, closest to the shoreline (45% small *vs.* 55% large), and So6 in the coconut grove (37% small *vs.* 63% large).

The underlying soils at Solano are devoid of foraminifera, but contain testate amoebae, except at the coconut grove sites (So12 and So13). Total concentrations of testate amoebae are generally higher in the soils of rice fields (5960–11,475 per 5 cm^3) than in the soils/sediments associated with grassy areas (135–280 per 5 cm^3), ponds (1250 per 5 cm^3), and coconut groves (0–65 per 5 cm^3). *Centropyxis* spp. dominates the grassy area between 260 m and 290 m (58%–70%), and beginning at 290 m inland, the assemblage switches to one that is dominated by *Difflugia* spp. (60%–93%).

5.4. Magay transect (Ma)

The surge height recorded at Magay on Leyte Island reached 5.4 m above MSL and 2.0 km inland (Soria et al., 2016b). However, we could only trace the deposit up to 1.7 km. The overwash sediments at Magay are characterized by a patchy, medium to fine sand (Soria et al., 2016a), variable thicknesses (<1–7 cm; Supplementary Table S4), a light brown color (10 YR 7/2), and the presence of siliciclastics and volcaniclastics. The contact between the overwash sediments and the underlying soil was sharp in the *Nypa* forest, but gradational at all other locations due to bioturbation by roots.

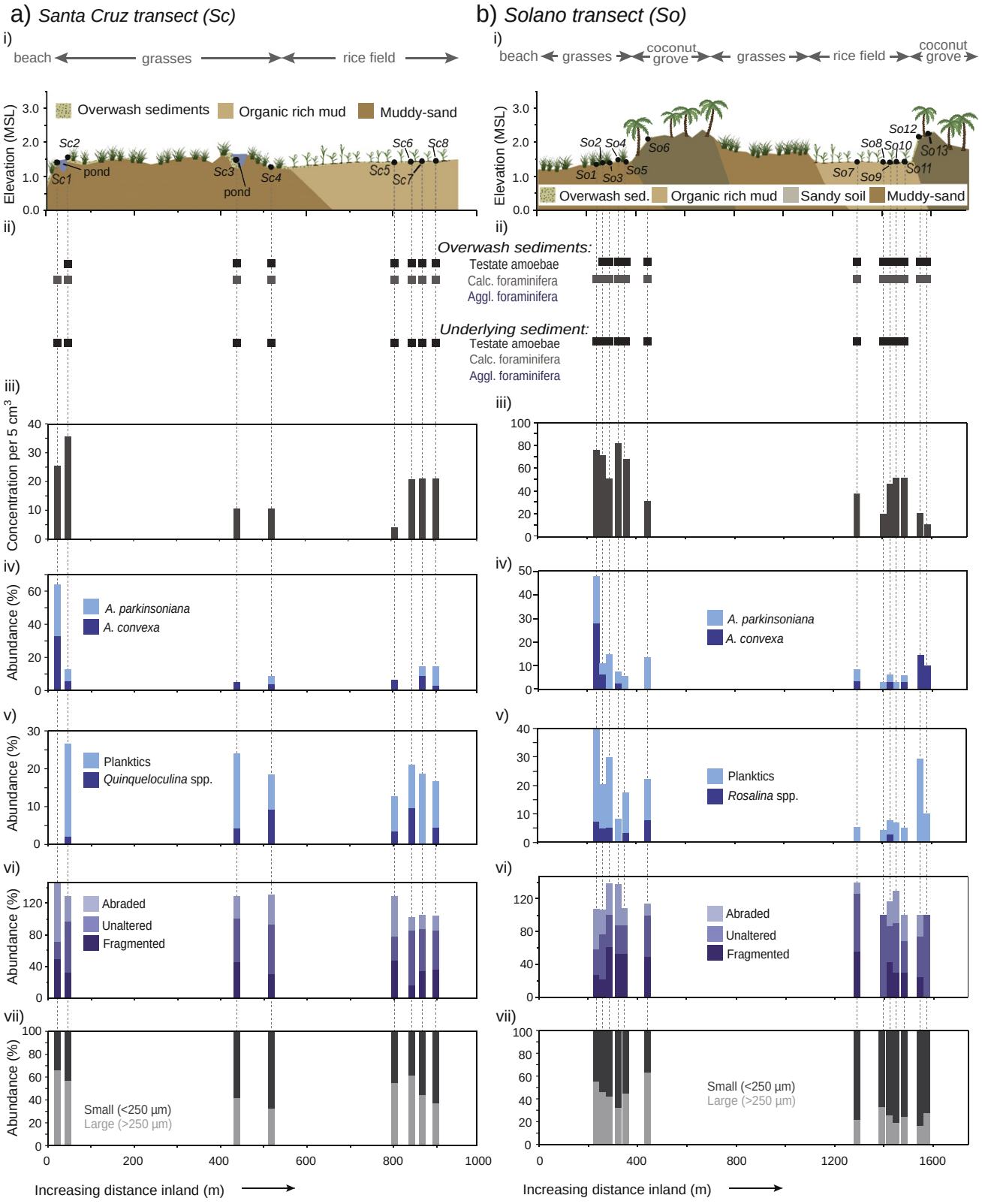

Fig. 4. Changes in the microfossil assemblage with increasing distance inland for (a) Sc (Santa Cruz) and (b) So (Solano). (i) Elevation schematic indicating major geomorphological features, location of sample sites (black circle), and thickness of the overwash sediments. (ii) Presence *vs.* absence of testate amoebae and foraminifera (calcareous and agglutinated) for each sample location. (iii) Concentration of foraminifera per 5 cm^3. (iv,v) Relative abundances of dominant foraminiferal species within the overwash sediments. (vi) Taphonomic condition of calcareous foraminifera. An individual foraminifera can be both abraded and fragmented. (vii) Abundances of small and large tests within the overwash sediments. Bar graphs are stacked histograms.

Foraminiferal concentrations within the overwash sediments at Magay are similar to those from Santa Cruz and Solano and range from 15 to 150 individuals per 5 cm^3 (Fig. 5a,b; Supplementary Table S4). The overwash sediments consist of benthic and planktic foraminifera that are both calcareous and agglutinated. In general, *Ammonia parkinsoniana* (6%–57%), and planktic species (0%–87%)

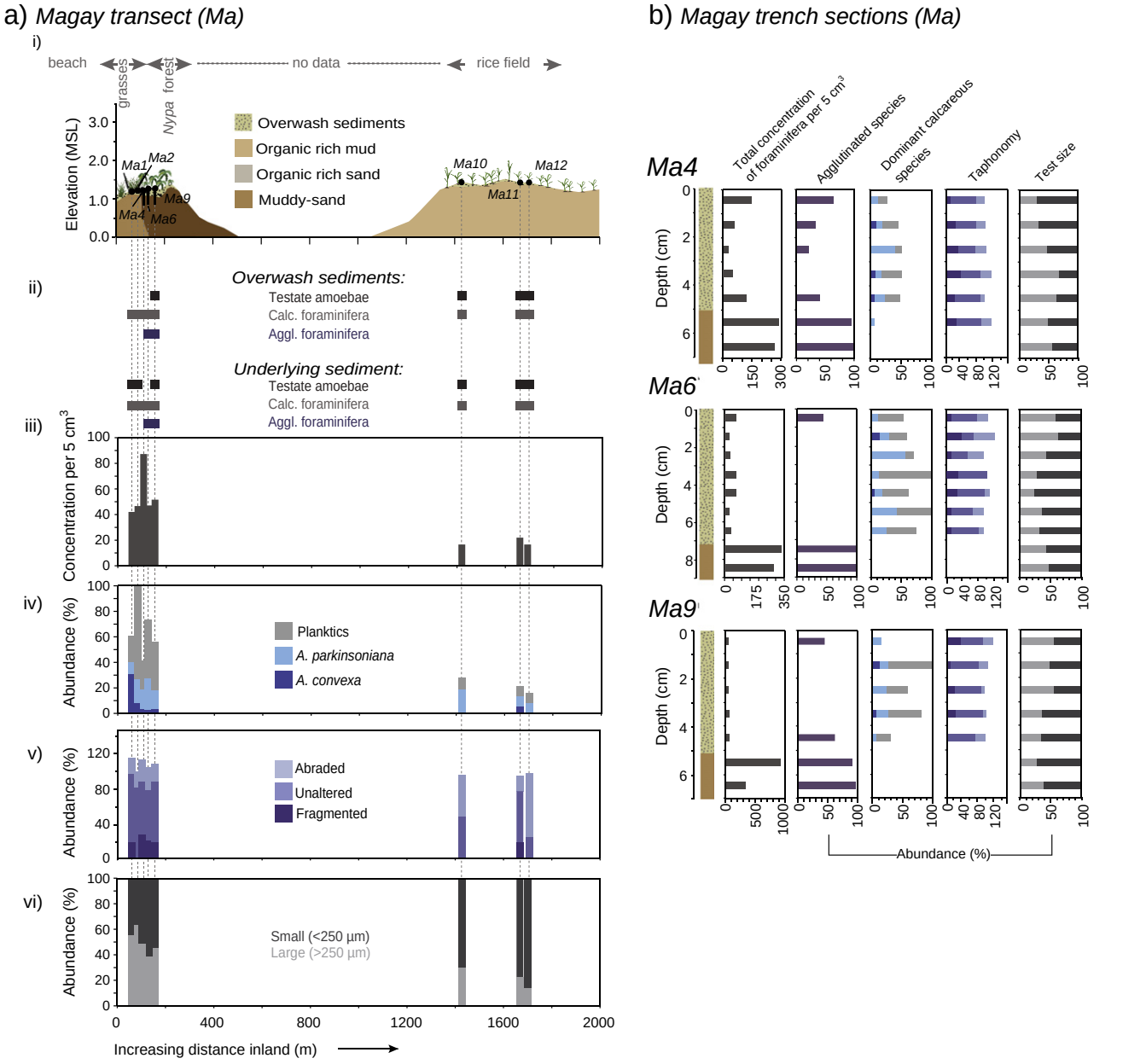

Fig. 5. (a) Changes in the microfossil assemblage with increasing distance inland for Ma (Magay). (i) Elevation schematic indicating major geomorphic features, locations of surface (black circle) and trench (thick black line) sample sites, and thickness of the overwash sediments. (ii) Presence *vs.* absence of testate amoebae and foraminifera (calcareous and agglutinated) for each sample location. (iii) Concentration of foraminifera per 5 cm^3. (iv) Relative abundances of dominant foraminiferal species within the overwash sediments. (v) Taphonomic condition of calcareous foraminifera. An individual foraminifera can be both abraded and fragmented. (vi) Abundances of small and large tests within the overwash sediments. The spatial gap between Ma9 and Ma10 corresponds to the village boundary where storm sediments accumulated over paved surfaces, but did not preserve (b) Trench sections (Ma4, Ma6, and Ma9) in the *Nypa* forest. Bar graphs are stacked histograms.

dominate the Haiyan assemblage. In contrast to all other sites, the Haiyan assemblage at Magay also contains agglutinated mangrove foraminifera. Agglutinated foraminifera are limited to sample locations within the *Nypa* forest (Ma4, Ma6, and Ma9; Supplementary Table S4) and include *Trochammina inflata* (Montagu, 1808; 0%–29%), *Miliammina fusca* (Brady, 1870; 0%–27%), *Haplophragmoides wilberti* Andersen, 1953 (0%–23%), *Entzia macrescens* (Brady, 1870; 0%–22%), and *Ammobaculites* sp. (0%–17%). Testate amoebae are also found within the overwash sediments at sites within the rice field, where *Difflugia* spp. dominate (37%–50%), as well as Ma9 (*Nypa* forest), where the testate amoebae assemblage of the overwash sediments is comprised exclusively of *Centropyxis* spp. (up to 27% of the total microfossil assemblage; Fig. 2). The taphonomic assemblage of the overwash sediments is dominated by unaltered individuals (29%–82%) up to a distance of 1.4 km inland, at which point the assemblage switches to one that is dominated by abraded forms (e.g., 75% of foraminifera at Ma12 are abraded). In general, the test size of foraminifera observed at Ma decreased with increasing distance inland (e.g., 64% large sized foraminifera at Ma2 *vs.* 14% at Ma12).

Soils underlying the *Nypa* forest (Ma4, Ma6, and Ma9) contained agglutinated foraminifera that comprised 90%–100% of the total microfossil assemblage (Fig. 5). Testate amoebae are present within underlying soils from the grassy area (69%–100% *Centropyxis* spp.), the rice fields (74%–76% *Difflugia* spp.), and to a lesser extent, within the *Nypa* (e.g., 4%–9% testate amoebae at Ma9). The trench stations at Ma4, Ma6, and Ma9 (sampled every 1 cm) show no relationship between total concentration and depth within the overwash sediments (Fig. 5b; Supplementary Table S4). However, concentrations were

significantly lower in the overwash sediments compared to the underlying soil (e.g., 35–70 *vs.* 325–905 foraminifera per 5 cm^3, respectively, at Ma9). The Haiyan assemblage in trench samples was dominated by planktic foraminifera (up to 87%), with agglutinated mangrove species found at the lower and upper contacts of the deposit. The taphonomic assemblage of the overwash sediments within trench sections was dominated by unaltered individuals (e.g., 50%–69% of the assemblage at Ma4), but did not show any relationship with depth. Test size showed a relationship with depth at trench Ma4, where larger foraminifera (>250 μm) were concentrated at the base of the overwash sediments (66% large at the base *vs.* 30% large at the top).

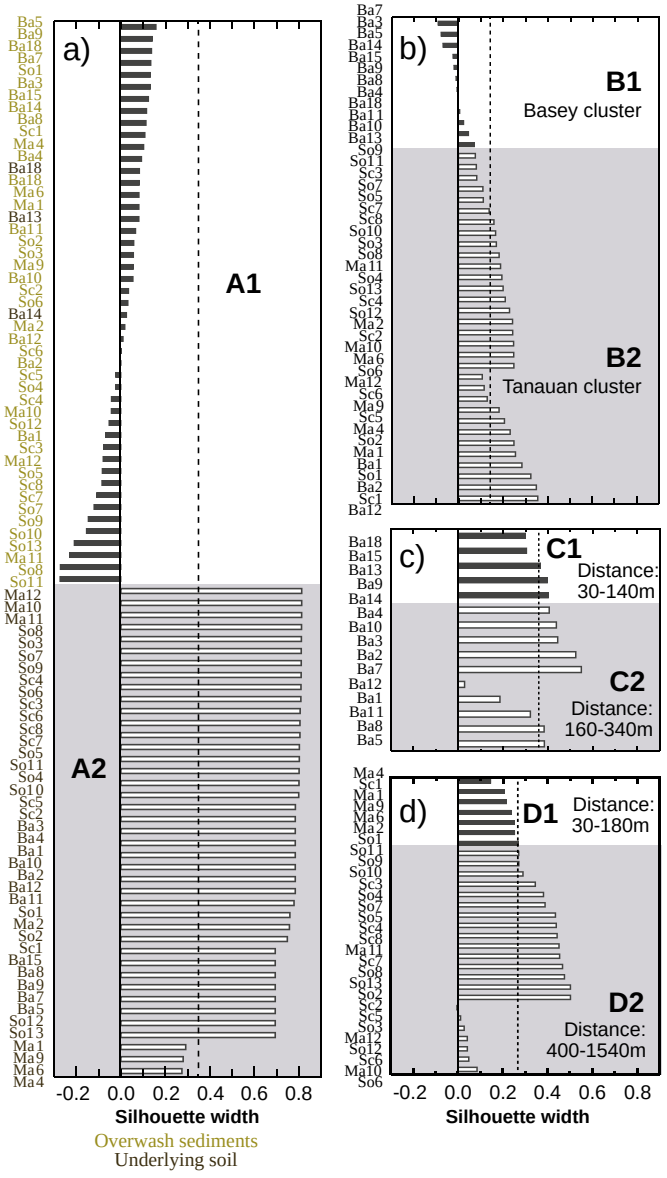

Fig. 6. Results of PAM cluster analysis indicating average silhouette width of clustered data. For each scenario, two clusters produced the highest average silhouette width (indicated by dashed vertical line) indicating that the data can be reliably divided into two clusters. (a) Discriminating between the overwash sediments and underlying sedimentary layer. Overwash sediment samples are indicated in yellow and underlying "pre-storm" sediments are indicated in brown. (b) Distinguishing between the overwash sediments at a mixed-carbonate site (Ba) and a clastic site (Sc, So, and Ma). Distance controlled clusters within overwash sediments at Ba (c) and the Tanauan transects (d). Distances from the shoreline for each cluster are indicated.

5.5. Cluster analysis

We used PAM cluster analysis to classify the microfossil signature of the overwash sediments and to assess lateral changes in the foraminiferal (relative abundance, total concentration, taxonomy, taphonomy, and test size) and testate amoebae data. PAM cluster analysis distinguished Haiyan sediments from the underlying soil (Fig. 6a). Cluster A1 (average silhouette width = 0.005) generally consisted of Haiyan sediments that are composed of calcareous foraminifera (5–6320 foraminifera per 5 cm^3); whereas cluster A2 (average silhouette width = 0.737) contained only underlying soil samples that were generally devoid of calcareous foraminifera. The underlying soils at Ba13, 14, and 18 clustered in A1 due to the presence of low abundances of calcareous foraminifera, which are common in Haiyan sediments (45–6320 foraminifera per 5 cm^3 at Ba).

PAM cluster analysis recognized two clusters corresponding to the overwash sediments derived from the mixed-carbonate environment of Basey (cluster B1) and the three clastic (cluster B2) transects from Tanauan (Fig. 6b). Cluster B1 (average silhouette width = 0.232) consists exclusively of Basey samples, which have high concentrations of calcareous foraminifera (45–6320 foraminifera per 5 cm^3) that were variably abraded and unaltered (19%–66% and 26%–64%, respectively). Cluster B2 (average silhouette width = 0.140) generally contained only Haiyan sediments derived from the clastic coastline near Tanauan. These samples are characterized by lower concentrations of calcareous foraminifera (5–80 foraminifera per 5 cm^3) that were generally more unaltered (e.g., 20%–82% at Ma) than those from cluster B1. The Haiyan sediments in Ba1, Ba2, and Ba12 clustered in B2 because of higher abundances of testate amoebae (63%, 35%, and 30%, respectively).

Two clusters within the overwash sediments at Basey (Ba) were defined based on their distance along the transect (Fig. 6c). Cluster C1 (average silhouette width = 0.261) corresponds to stations within 140 m of the shoreline, and cluster C2 (average silhouette width = 0.414) corresponds to samples from distances ranging from 160 to 340 m. The clusters were generally defined by the presence of testate amoebae (0 testate amoebae per 5 cm^3 in C1 *vs.* up to 535 per 5 cm^3 in C2), and small foraminifera (29%–57% (average = 41%) in C1 *vs.* 39%–100% (average = 82%) in C2). PAM cluster analysis of the three Tanauan transects (Sc, So, and Ma) produced two clusters: D1 (average silhouette width = 0.040) corresponding to stations within 180 m of the shoreline, and D2 (average silhouette width = 0.350), corresponding to distances ranging from 400 to 1540 m (Fig. 6d). The overwash sediments at stations in cluster D1 are characterized by the presence of agglutinated foraminifera (up to 97 individuals per 5 cm^3), the absence or low abundance of testate amoebae (absent except at Ma9 where, up to 15 individuals of *Centropyxis* spp. were found), and large foraminifera (39%–66%; average = 53%). In contrast, the overwash sediments at stations in cluster D2 are characterized by a paucity of agglutinated foraminifera, higher concentrations of testate amoebae (10–440 testate amoebae per 5 cm^3), and higher abundances of small foraminifera (37%–86%; average = 64%).

6. Microfossil characteristics of the Haiyan overwash sediments

The sediments deposited by Typhoon Haiyan on coastlines of the Leyte Gulf were discriminated from underlying sediments (e.g., clusters A1 and A2 on Fig. 6a) based on the presence of intertidal and subtidal benthic, and planktic foraminifera. At three of the four sites (Basey, Santa Cruz, and Solano), calcareous species were the main constituents of the foraminiferal assemblage (up to 6320 foraminifera per 5 cm^3), but were generally absent in underlying soils. This was especially clear with samples collected from the Tanauan transects where there was a paucity of calcareous foraminifera in underlying soils (except at Ma4), but up to 97 individuals per 5 cm^3 in the overwash sediments. This trend is in agreement with other studies that have documented overwash

sediments in coastal settings and have found influxes and increased diversity of marine foraminifera within storm deposits (Hippensteel and Martin, 1999; Cochran et al., 2005; Hawkes and Horton, 2012).

Although the Haiyan overwash sediments could be easily discriminated from the underlying soils at all sites, the contrasting environments between Basey and the Tanauan transects resulted in differing microfossil assemblages and two distinct PAM-defined clusters (B1: Haiyan overwash sediments from Basey; B2: Haiyan overwash sediments from Tanauan; Fig. 6b). For example, in the Tanauan transects (Sc, So, and Ma), the foraminiferal assemblage consists of 35%–100% calcareous species, with *A. parkinsoniana* and planktics dominating (at Ma, up to 57% and 87%, respectively). At Basey (Ba), a protected carbonate tidal flat, the overwash sediments contained abundant and diverse foraminifera that are exclusively calcareous and include typical intertidal (e.g., *A. parkinsoniana*, *A. tepida*), subtidal (e.g., *Cibicides* sp., *Pararotalia* sp.), and planktic species. Mixed assemblages, containing nearshore benthics as well as offshore planktics, have been reported in association with storm and tsunami sediments (e.g., Dahanayake and Kulasena, 2008; Uchida et al., 2010; Hawkes and Horton, 2012; Pilarczyk et al., 2012). For example, Uchida et al. (2010) found a mixture of shallow- (0–30 m water depth) and deep-dwelling (>170 m water depth) benthics, and planktic foraminifera within tsunami sediments from Japan. Similarly, overwash sediments associated with the 2004 Indian Ocean tsunami were composed of a mixed foraminiferal assemblage containing shallow intertidal, nearshore, and planktic taxa (Nagendra et al., 2005; Hawkes et al., 2007). At all sample locations, planktic species are a main constituent of the Haiyan overwash sediments, with highest abundances found in Haiyan sediments from Tanauan (e.g., up to 87% at Ma). Planktic foraminifera are commonly found in overwash sediments and have previously been used to identify and interpret storm deposits (e.g., Hippensteel and Martin, 1999; Hawkes and Horton, 2012). The presence of planktic foraminifera up to the landward limit of the overwash sediments may be related to their small size and chamber arrangement, which is designed for floatation in the water column (BouDagher-Fadel et al., 1997).

In addition to influxes of calcareous foraminifera, the Haiyan overwash sediments could be identified by the presence of intertidal agglutinated species (up to 97 per 5 cm^3) at Magay. Agglutinated intertidal foraminifera (e.g., *E. macrescens*, *M. fusca*, and *T. inflata*), characteristic of salt marsh and mangrove environments (Culver, 1990; Woodroffe et al., 2005), were sourced from the soils underlying the *Nypa* forest and incorporated into the overwash sediments at Magay. Agglutinated mangrove foraminifera, such as those found within the Haiyan overwash sediments, have also been found in association with tsunami sediments elsewhere (Onuki et al., 1961; Nagendra et al., 2005; Hawkes et al., 2007) and indicate scour of coastal sediments by large waves. In trench sections, the concentration of agglutinated taxa within the overwash sediments peaked in the upper 1 cm, possibly indicating rapid recolonization of foraminifera following the typhoon (Horton et al., 2009).

Although testate amoebae have been used to identify freshwater environments (e.g., Charman, 2001, Scott et al., 2001), they have not been used to distinguish overwash sediments. Within our study area, testate amoebae are abundant in underlying rice field soils (up to 11,475 individuals per 5 cm^3), ponds (up to 1250 individuals per 5 cm^3), and grassy areas (up to 280 individuals per 5 cm^3), with coconut groves being nearly devoid of them. Taxa such as *Difflugia* spp. and *Centropyxis* spp. were a component of the Haiyan assemblage at locations where the underlying soil contained abundant testate amoebae (e.g., Ba1–Ba4, Ba10–Ba12; Fig. 3a,b). Species of *Difflugia* are common in sediments from freshwater environments such as lakes, bogs, and ponds (Medioli and Scott, 1983). Species of *Centropyxis* often have a higher salinity tolerance and their ecological niche spans both freshwater and brackish environments (e.g., Scott et al., 2001). In general, *Difflugia* spp. dominated inland rice field soils at our sites. Abundances of *Centropyxis* spp. increased in grassy soils and pond sediments that were located closer to the coastline and influenced by periodic marine inundation and salt spray.

Calcareous foraminifera within the overwash sediments were generally larger in size (up to 71% of the assemblage was >250 μm) compared to those from the underlying soils. The size of individual foraminifera can be used to assess the transport history of coastal sediments (e.g., Li et al., 1998; Yordanova and Hohenegger, 2007; Pilarczyk and Reinhardt, 2012). This technique has recently been applied to overwash sediments (e.g., Hawkes et al., 2007; Uchida et al., 2010) on the basis that test size, similar to sediment grain size, is an indicator of change in energy and distance of transport (e.g., Weiss, 2008).

Changes in the abundance of large and small test sizes contributed to defining two clusters corresponding to distance from the shoreline (Fig. 6c, d). In general, the test size of calcareous foraminifera within the overwash sediments varied with distance inland. This trend was most pronounced at Basey where an assemblage shift from large tests (>250 μm) to small tests occurred at ~150 m (Fig. 3; Supplementary Table S1). Similarly, test size decreased with increasing distance inland at Solano and Magay (Figs. 4, 5; Supplementary Tables S2-S4). For example, the assemblage decreased from 56% large foraminifera closest to the shoreline at Magay to 14% at the landward limit of the overwash sediments. This is similar to a study by Pilarczyk et al. (2012) that documented a landward decrease in test size within the Tohoku tsunami sediments from Sendai, Japan. The decrease in test size within the Tohoku tsunami sediments coincided with the introduction of mud into the sand deposit, which was a result of the waning energy and sustained pooling of marine water. At Santa Cruz, test size decreased from 66% closest to the shoreline to 36% at the most landward extent of the transect. However, anomalously high abundances of large tests were found at Sc5–Sc6 (57% and 61%, respectively) and may be the result of pooling storm surge water in low-lying areas within the rice field.

7. Provenance of the Haiyan overwash sediments

Sediments deposited by Typhoon Haiyan on coastlines of the Leyte Gulf contain microfossils of subtidal, intertidal, and freshwater origin. This is to be expected, because as typhoons approach a coastline, they erode, transport, and deposit marine, coastal, and terrigenous sediments (Hawkes and Horton, 2012; Hippensteel et al., 2013; Pilarczyk et al., 2014). The presence of foraminifera of intertidal to subtidal origin suggests that a major component of the overwash sediments was derived from shallow nearshore locations, with the possibility of a deeper source. For example, at Basey, the overwash sediments were sourced predominantly from intertidal to subtidal (*A. parkinsoniana*, *A. tepida*) sediments along a protected mixed-carbonate coastline. However, the overwash sediments also contained up to 13% of unaltered deeper-dwelling (up to 60 m water depth; Javaux and Scott, 2003) *E. repandus*, *C. tabaensis*, and planktics. The presence of these taxa indicates that the storm surge scoured not only the nearshore but also potentially deeper sediments. Deeper-dwelling microfossils have previously been found in overwash deposits (e.g., Hawkes et al., 2007; Uchida et al., 2010; Lane et al., 2011; Sieh et al., 2015) and assist to understand the sources for both storm and tsunami sediments. Lane et al. (2011) used offshore surface transects to assess the species ecology of foraminifera from northwestern Florida to estimate a minimum depth of scour by storm for overwash sediments within a sinkhole. Offshore species of foraminifera have been reported in nearshore sediments; however, they are typically abraded and corroded and not unaltered like those found within the Haiyan overwash sediments (e.g., Glenn-Sullivan and Evans, 2001; Pilarczyk et al., 2011).

Intertidal agglutinated foraminifera (ranging from 0% to 65% of the assemblage) and testate amoebae (ranging from 0% to 93% of the assemblage) were also found within the overwash sediments. Due to their extensive habitat range (Scott et al., 2001), which spans intertidal and virtually all inland aquatic environments (e.g., Charman, 2001), testate amoebae, combined with intertidal agglutinated foraminifera, can

assist to identify storm overwash sediments because their presence indicates terrestrial scour, transport, and mixing by the storm surge. For example, Hawkes et al. (2007) used agglutinated mangrove foraminifera contained within the 2004 Indian Ocean tsunami sediments to identify backwash.

The taphonomic (or surface) character of individual foraminifera (e.g., size and patterns of abrasion, corrosion, and fragmentation) has been used to assess sediment provenance (e.g., Pilarczyk and Reinhardt, 2012) and, when applied to overwash sediments, can provide insight into depth of scour and size of event (e.g., Sieh et al., 2015). Storm and tsunami sediments often contain relatively high abundances of unaltered foraminifera (e.g., Satyanarayana et al., 2007; Goff et al., 2011; Pilarczyk et al., 2012; Sieh et al., 2015) because they scour and deposit marine sediment from protected subtidal locations. Foraminifera within the Haiyan overwash sediments are predominantly unaltered (e.g., up to 64% at Basey and up to 100% at Solano), suggesting that their main source was not from an exposed beach or shallow intertidal areas, which would be dominated by corroded and abraded individuals (Glenn-Sullivan and Evans, 2001; Pilarczyk et al., 2012). In an example from a carbonate reef coastline in the Philippines, Glenn-Sullivan and Evans (2001) found that abraded foraminifera were twice as abundant as unaltered individuals in the shallow areas (<5 m of water depth). Given the shallow, gently-sloping tidal flat at Basey, and the high abundances of unaltered foraminifera (up to 64% of the taphonomic assemblage) within the overwash sediments, the storm surge must have scoured and transported sediment from further offshore where water depths exceed 5 m.

8. Conclusions

In January 2014, two months after Typhoon Haiyan made landfall on the Philippines, we documented the microfossil assemblages within the resulting overwash sediments. Foraminiferal assemblages were used to distinguish the overwash sediments from underlying soils based predominantly on the presence of calcareous foraminifera such as shallow benthic species and planktics. In general, underlying soils did not contain calcareous foraminifera, but rather, were characterized by higher abundances of testate amoebae.

The Haiyan microfossil assemblage also provided information regarding sediment provenance. PAM cluster analysis subdivided the Haiyan microfossil dataset into two assemblages based on depositional environment: (1) a low-energy mixed-carbonate tidal flat located on Samar Island (Basey transect); and (2) a higher-energy clastic coastline near Tanauan on Leyte Island (Santa Cruz, Solano, and Magay transects). Testate amoebae (e.g., *Centropyxis* spp., *Difflugia* spp.) and foraminifera (e.g., *A. parkinsoniana*, *A. tepida*) contained within overwash sediments at each of the transects reveal up to three dominant sources for the overwash sand: terrestrial, intertidal, and subtidal sources. At Basey, we infer a fourth source, subtidal locations deeper than 5 m, based on the presence of taphonomically unaltered deeper-dwelling species such as *E. repandus*, *C. tabaensis*, and planktics. The presence of agglutinated mangrove foraminifera and freshwater testate amoebae within the overwash sediments indicates scouring, mixing, and transport of terrestrial and brackish intertidal sediments by the storm surge.

The addition of taphonomic and test size data confirmed taxonomic results that indicate a mixed source for the Haiyan overwash sediments. High abundances of unaltered foraminifera within the overwash sediments suggest that the main source of sediment was not from exposed intertidal areas, but rather, from protected subtidal locations in excess of 5 m of water depth.

Supplementary data to this article can be found online at http://dx.doi.org/10.1016/j.sedgeo.2016.04.001.

Acknowledgements

The authors would like to thank Jane Mercado (Santa Cruz), Jiggo Bermiso (Magay), Carmelita Villamor (Solano), and Pelagio Tecson Jr. (Mayor of Tanauan) who granted permission to conduct fieldwork on their land. Stephen Carson assisted with laboratory analyses. The authors thank Jasper Knight, Briony Mamo, and an anonymous reviewer for their insightful comments that improved the manuscript. This work comprises Earth Observatory of Singapore contribution no. 110. This research is supported by the National Science Foundation (EAR 1418717), the National Research Foundation Singapore (National Research Fellow Award No. NRF-RF2010-04), and the Singapore Ministry of Education under the Research Centers of Excellence initiative.

References

Allen, C.R., 1962. Circum-Pacific faulting in the Philippines–Taiwan region. Journal of Geophysical Research 67, 4795–4812.
Andersen, H.V., 1953. Two new species of *Haplophragmoides* from the Louisiana coast. Cushman Foundation for Foraminiferal Research Contribution 4, Washington, D.C. (21 pp.)
BouDagher-Fadel, M.K., Banner, F.T., Whittaker, J.E., 1997. Early Evolutionary History of Planktonic Foraminifera. British Micropalaeontological Society, London (269 pp.).
Brady, H.B., 1870. An analysis and description of the foraminifera. In: Brady, G.S., Robertson, D. (Eds.), The Ostracodes and Foraminifera of Tidal Rivers v. 6., Annals and Magazine of Natural History, London, England (500 pp.).
Brandon, C.M., Woodruff, J.D., Lane, D.P., Donnelly, J.P., 2013. Tropical cyclone wind speed constraints from resultant storm surge deposition: a 2500 year reconstruction of hurricane activity from St. Marks, FL. Geochemistry, Geophysics, Geosystems 14, 2993–3008.
Charman, D.J., 2001. Biostratigraphic and palaeoenvironmental applications of testate amoebae. Quaternary Science Reviews 20, 1753–1764.
Clark, K., Cochran, U., Mazengarb, C., 2011. Holocene coastal evolution and evidence for paleotsunami from a tectonically stable region, Tasmania, Australia. The Holocene 21, 883–895.
Cochran, U.A., Berryman, K.R., Middlenhall, D.C., Hayward, B.W., Southall, K., Hollis, C.J., 2005. Towards a record of Holocene tsunami and storms from Northern Hawke's Bay, New Zealand. New Zealand Journal of Geology and Geophysics 48, 507–515.
Collins, A.C., 1958. Foraminifera. Great Barrier Reef Expedition 1928–1929. Scientific Reports vol. 6. British Museum of Natural History, London (414 pp.).
Collins, E.S., Scott, D.B., Gayes, P.T., 1999. Hurricane records on the South Carolina coast: can they be detected in the sediment record? Quaternary International 56, 15–26.
Culver, S.J., 1990. Benthic foraminifera of Puerto Rican mangrove–lagoon systems: potential for palaeoenvironmental interpretations. Palaios 5, 34–51.
Cushman, J.A., 1926. Recent Foraminifera from Puerto Rico. Carnegie Institute Washington, Publication no. 344, Washington, D.C. (344 pp.).
d'Orbigny, A., 1839. Foraminiferes. In: de la Sagra, R. (Ed.), Histoire physique et naturelle de l'Ile de Cuba. A. Bertrand, Paris, France (454pp.).
Dahanayake, K., Kulasena, N., 2008. Recognition of diagnostic criteria for recent- and paleo-tsunami sediments from Sri Lanka. Marine Geology 254, 180–186.
Debenay, J.-P., 2013. A guide to 1,000 foraminifera from Southwestern Pacific, New Caledonia. IRD Éditions. Publications scientifiques du Muséum national d'Histoire naturelle, Paris, France (384 pp.).
Denommee, K.C., Bentley, S.J., Droxler, A.W., 2014. Climatic controls on hurricane patterns: a 1200-y near-annual record from Lighthouse Reef, Belize. Scientific Reports 4, 3876. http://dx.doi.org/10.1038/srep03876.
Dominey-Howes, D., Cundy, A., Croudace, I., 2000. High energy marine flood deposits on Astypalaea Island, Greece: possible evidence for the AD 1956 southern Aegean tsunami. Marine Geology 163, 303–315.
Donnelly, J.P., Hawkes, A.D., Lane, P., MacDonald, D., Shuman, B.N., Toomey, M.R., van Hengstum, P.J., Woodruff, J.D., 2015. Climate forcing of unprecedented intense-hurricane activity in the last 2000 years. Earth's Future 3, 49–65.
Donnelly, J.P., Roll, S., Wengren, M., Butler, J., Lederer, R., Webb, T., 2001. Sedimentary evidence of intense hurricane strikes from New Jersey. Geology 29, 615–618.
Duquesnoy, T., Barrier, E., Kasser, M., Aurelio, M.A., Gaulon, R., Punongbayan, R.S., Rangin, C., 1994. Detection of creep along the Philippine Fault: first results of geodetic measurements on Leyte Island, central Philippine. Geophysical Research Letters 21, 975–978.
Fichtel, L., Moll, J.P.C., 1798. Testacea microscopica aliaque minuta ex generibus *Argonauta* et *Nautilus* (Microscopische und andere kleine Schalthiere aus den Geschlechtern Argonaute und Schiffer). Anton Pichler, Vienna (124pp.).
Garcia-Herrera, R., Ribera, P., Hernandez, E., Gimeno, L., 2007. Northwest Pacific typhoons documented by the Philippine Jesuits, 1566–1900. Journal of Geophysical Research 112, D06108. http://dx.doi.org/10.1029/2006JD007370.
Glenn-Sullivan, E.C., Evans, I., 2001. The effects of time-averaging and taphonomy on the identification of reefal sub-environments using larger foraminifera: Apo Reef, Mindoro, Philippines. Palaios 16, 399–408.
Goff, J., Lamarche, G., Pelletier, B., Chagué-Goff, C., Strotz, L., 2011. Predecessors to the 2009 South Pacific tsunami in the Wallis and Futuna archipelago. Earth-Science Reviews 107, 91–106.
Hart, J., Hearn, G., Chant, C., 2002. Engineering on the precipice: mountain road rehabilitation in the Philippines. Quaternary Journal of Engineering Geology and Hydrogeology 35, 223–231.
Hawkes, A.D., Horton, B.P., 2012. Sedimentary record of storm deposits from Hurricane Ike, Galveston and San Luis Islands, Texas. Geomorphology 171, 180–189.
Hawkes, A.D., Bird, M., Cowie, S., Grund-Warr, C., Horton, B.P., Shau Hwai, A.T., Law, L., Macgregor, C., Nott, J., Ong, J.E., Rigg, J., Robinson, R., Tan-Mullins, M., Tiong Sa, T.,

Yasin, Z., Aik, L.W., 2007. Sediments deposited by the 2004 Indian Ocean tsunamis along the Malaysia–Thailand Peninsula. Marine Geology 242, 169–190.
Hayward, B.W., Holzmann, M., Grenfell, H.R., Pawlowski, J., Triggs, C.M., 2004. Morphological distinction of molecular types in *Ammonia*—towards a taxonomic revision of the world's most commonly misidentified foraminifera. Marine Micropaleontology 50, 237–271.
Hewins, M.R., Perry, C.T., 2006. Bathymetric and environmentally influenced patterns of carbonate sediment accumulation in three contrasting reef settings, Danjugan Island, Philippines. Journal of Coastal Research 22, 812–824.
Hippensteel, S.P., Martin, R.E., 1999. Foraminifera as an indicator of overwash deposits, barrier island sediment supply, and barrier island evolution: Folly Island, South Carolina. Palaeogeography Palaeoclimatology Palaeoecology 149, 115–125.
Hippensteel, S.P., Eastin, M.D., Garcia, W.J., 2013. The geological legacy of Hurricane Irene: implications for the fidelity of the paleo-storm record. GSA Today 23, 4–10.
Hippensteel, S.P., Martin, R.E., Harris, M.S., 2005. Discussion: records of prehistoric hurricanes on the South Carolina coast based on micropaleontological and sedimentological evidence, with comparison to other Atlantic Coast records. Geological Society of America Bulletin 117, 250–256.
Horton, B.P., Rossi, V., Hawkes, A.D., 2009. The sedimentary record of the 2005 hurricane season from the Mississippi and Alabama coastlines. Quaternary International 195, 15–30.
Javaux, E.J., Scott, D.B., 2003. Illustration of modern benthic foraminifera from Bermuda and remarks on distribution in other subtropical/tropical areas. Palaeontologia Electronica 6 (22 pp., http://palaeo-electronica.org/2003_1/benthic/issue1_03.htm.).
Joint Typhoon Warning Center, 2014. JTWC Western North Pacific best track data 2013. Available online at http://www.usno.navy.mil/NOOC/nmfcph/RSS/jtwc/best_tracks/wpindex.php.
Kaufman, L., Rousseeuw, P.J., 1990. Finding Groups in Data: An Introduction to Cluster Analysis. Wiley-Interscience, California (368 pp.).
Kemp, A.C., Horton, B.P., Vann, D.R., Engelhart, S.E., Grand Pre, C.A., Vane, C.H., Nikitina, D., Anisfeld, S.C., 2012. Quantitative vertical zonation of salt-marsh foraminifera for reconstructing former sea level: an example from New Jersey, USA. Quaternary Science Reviews 54, 26–39.
Kortekaas, S., Dawson, A.G., 2007. Distinguishing tsunami and storm deposits: an example from Martinhal, SW Portugal. Sedimentary Geology 200, 208–221.
Lacuna, M.L.D.G., Alviro, M.P., 2014. Diversity and abundance of benthic foraminifera in nearshore sediments of Iligan City, Northern Mindanao, Philippines. ABAH Bioflux 6, 10–26.
Lacuna, M.L.D.G., Masangcay, S.I.G., Orbita, M.L.S., Torres, M.A.J., 2013. Foraminiferal assemblage in southeast coast of Iligan Bay, Mindanao, Philippines. AACL Bioflux 6, 303–319.
Landsea, C.W., Harper, B.A., Hoarau, K., Knaff, J.A., 2006. Can we detect trends in extreme tropical cyclones? Science 313, 452–454.
Lane, P., Donnelly, J.P., Woodruff, J.D., Hawkes, A.D., 2011. A decadally-resolved paleohurricane record archived in the late Holocene sediments of a Florida sinkhole. Marine Geology 287, 14–30.
Li, C., Jones, B., Kalbfleisch, W.B.C., 1998. Carbonate sediment transport pathways based on foraminifera: case study from Frank Sound, Grand Cayman, British West Indies. Sedimentology 45, 109–120.
Lin, I.I., Black, P., Price, J.F., Yang, C.-Y., Chen, S.S., Lien, C.-C., Harr, P., Chi, N.-H., Wu, C.-C., D'Asaro, E.A., 2013. An ocean coupling potential intensity index for tropical cyclones. Geophysical Research Letters 40, 1878–1882.
Liu, K.B., Fearn, M.L., 1993. Lake-sediment record of late Holocene hurricane activities from coastal Alabama. Geology 21, 793–796.
Liu, K.B., Fearn, M.L., 2000. Reconstruction of prehistoric landfall frequencies of catastrophic hurricanes in northwestern Florida from lake sediment records. Quaternary Research 54, 238–245.
Loeblich, A.R., Tappan, H., 1987. Foraminiferal genera and their classification. Van Nostrand Rienhold Co., New York, pp. I–II.
Maechler, M., Rousseeuw, P., Struyf, A., Hubert, M., 2005. Cluster Analysis Basics and Extensions. Available at: URL http://cran.r-project.org/web/packages/cluster/index.html.
Medioli, F.S., Scott, D.B., 1983. Holocene Arcellacea (Thecamoebians) from Eastern Canada. Cushman Foundation for Foraminiferal Research Special Publication 21 pp. 1–63.
Montagu, G., 1808. Supplement to Testacea Britannica. Exeter, England (81 pp.).
Mori, N., Kato, M., Kim, S., Mase, H., Shibutani, Y., Takemi, T., Tsuboki, K., Yasuda, T., 2014. Local amplification of storm surge by super typhoon Haiyan in Leyte Gulf. Geophysical Research Letters 41, 5106–5113.
Nagendra, R., Kannan, B.V.K., Sajith, C., Sen, G., Reddy, A.N., Srinivasalu, S., 2005. A record of foraminiferal assemblage in tsunami sediments along Nagappattinam coast, Tamil Nadu. Current Science 89, 1947–1952.
NDRRMC (National Disaster Risk Reduction and Management Council), 2014u. SitRep No. 27 Effects of Typhoon "Ruby" (Hagupit), 19 December 2014. Available at: www.ndrrmc.gov.ph.
Nguyen, P., Sellars, S., Thorstensen, A., Tao, Y., Ashouri, H., Braithwaite, D., Hsu, K., Sorooshian, S., 2014. Satellites track precipitation of Super Typhoon Haiyan. EOS Transactions 95, 133–135.
Ogden, C.G., Hedley, R.H., 1980. An atlas of freshwater testate amoebae. Oxford University Press, New York (222 pp.).
Onuki, Y., Shibata, T., Mii, H., 1961. Coastal region between Taro and Kamaishi. In: Kon'no, E. (Ed.), Geological observations of the Sanriku coastal region damaged by the tsunami due to the Chile earthquake in 1969. Contributions from the Institute of Geology and Paleontology. Tohoku University, Sendai, pp. 16–27.
Otvos, E.F., 1999. Quaternary coastal history, basin geometry and assumed evidence for hurricane activity, northeastern Gulf of Mexico coastal plain. Journal of Coastal Research 15, 438–443.
Perelis, L., Reiss, Z., 1976. Cibicididae. Recent sediments from the Gulf of Elat. Israel Journal of Earth Science, Jerusalem, Israel 24 (78 pp.).
Pilarczyk, J.E., Reinhardt, E.G., 2012. *Homotrema rubrum* (Lamarck) taphonomy as in overwash indicator in Marine Ponds on Anegada, British Virgin Islands. Natural Hazards 63, 85–100.
Pilarczyk, J.E., Dura, T., Horton, B.P., Engelhart, S.E., Kemp, A.C., Sawai, Y., 2014. Microfossils from coastal environments as indicators of paleo-earthquakes, tsunamis and storms. Palaeogeography, Palaeoclimatology, Palaeoecology 413, 144–157.
Pilarczyk, J.E., Horton, B.P., Witter, R.C., Vane, C.H., Chagué-Goff, C., Goff, J., 2012. Sedimentary and foraminiferal evidence of the 2011 Tohoku-oki tsunami on the Sendai coastal plain, Japan. Sedimentary Geology 282, 78–89.
Pilarczyk, J.E., Reinhardt, E.G., Boyce, J.I., Schwarcz, H.P., Donato, S.V., 2011. Assessing surficial foraminiferal distributions as an overwash indicator in Sur Lagoon, Sultanate of Oman. Marine Micropaleontology 80, 62–73.
Pun, I.-F., Lin, I.-I., Lo, M.-H., 2013. Recent increase in high tropical cyclone heat potential area in the Western North Pacific Ocean. Geophysical Research Letters 40, 4680–4684.
Rabien, K.A., Culver, S.J., Buzas, M.A., Corbett, D.R., Walsh, J.P., Tichenor, H.R., 2015. The foraminiferal signature of recent Gulf of Mexico hurricanes. Journal of Foraminiferal Research 45, 82–105.
Ribera, P., Garcia-Herrera, R., Gimeno, L., 2008. Historical deadly typhoons in the Philippines. Weather 63, 194–199.
Satyanarayana, K., Reddy, A.N., Jaiprakash, B.C., Chidambaram, L., Srivastava, S., Bharktya, D.K., 2007. A note on foraminifera, grain size and clay mineralogy of tsunami sediments from Karaikal-Nagore-Nagapattiuam Beaches, Southeast Coast of India. Journal of the Geological Society of India 69, 70–74.
Scott, D.B., Collins, E.S., Gayes, P.T., Wright, E., 2003. Records of prehistoric hurricanes on the South Carolina coast based on micropaleontological and sedimentological evidence, with comparison to other Atlantic Coast records. Geological Society of America Bulletin 115, 1027–1039.
Scott, D.B., Medioli, F.S., Schafer, C.T., 2001. Monitoring in Coastal Environments Using Foraminifera and Thecamoebian Indicators. Cambridge University Press, Cambridge (177pp.).
Sieh, K., Daly, P., McKinnon, E.E., Pilarczyk, J.E., Chiang, H.W., Horton, B., Rubin, C.M., Shen, C.C., Ismail, N., Vane, C.H., Feener, R.M., 2015. Penultimate predecessors of the 2004 Indian Ocean tsunami in Aceh, Sumatra: Stratigraphic, archeological, and historical evidence. Journal of Geophysical Research—Solid Earth 120, 308–325.
Smith, H.G., Bobrov, A., Lara, E., 2008. Diversity and biogeography of testate amoebae. Biodiversity and Conservation 17, 329–343.
Soria, J.L.A., Switzer, A.D., Pilarczyk, J.P., Siringan, F.P., Doctor, A., Khan, N., Fritz, H.M., Ramos, R.D., Ildefonso, S.R., Garcia, M., 2016a. Sedimentary record of the 2013 Typhoon Haiyan deposit in the Leyte Gulf, Philippines. European Geosciences Union (EGU) Meeting, Vienna, Austria (2016, abstract #EGU2016-260).
Soria, J.L.A., Switzer, A.D., Villanoy, C.L., Fritz, H.M., Bilgera, P.H.T., Cabrera, O.C., Siringan, F.P., Yacat-Sta. Maria, Y., Ramos, R.D., Fernandez, I.Q., 2016b. Repeat storm surge disasters of Typhoon Haiyan and its 1897 predecessor in the Philippines. Bulletin of the American Meteorological Society 97, 31–48.
Strotz, L.C., Mamo, B.L., 2009. Can foraminifera be used to identify storm deposits in shallow-water tropical reef settings? Examining the impact of Cyclone Hamish on the foraminiferal assemblages of Heron Island, Great Barrier Reef, Australia. American Geophysical Union, Fall Meeting (2009, abstract #NH43B-1311).
Suerte, L.O., Yumul Jr., G.P., Tamayo Jr., R.A., Dimalanta, C.B., Zhou, M.-F., Maury, R.C., Polvé, M., Balce, C.L., 2005. Geology, Geochemistry and U-Pb SHRIMP age of the Tacloban Ophiolite Complex, Leyte (Central Philippines): implications for the existence and extent of the Proto-Philippine Sea Plate. Resource Geology 55, 207–216.
Tajima, Y., Yasuda, T., Pacheco, B.M., Cruz, E.C., Kawasaki, K., Nobuoka, H., Miyamoto, M., Asano, Y., Arikawa, T., Ortigas, N.M., Aquino, R., Mata, W., Valdez, J., Briones, F., 2014. Initial report of JSCE-PICE joint survey on the storm surge disaster caused by Typhoon Haiyan. Coastal Engineering Journal 56, 1450006. http://dx.doi.org/10.1142/S0578563414500065.
Travaglia, C., Baes, A.F., Tomas, L.M., 1978. Geology of Samar Island: Annex 6 of Samar Island Reconnaissance Land Resources Survey of Priority Strips for Integrated Rural Development. United Nations Development Programme, Manila (149pp.).
Uchida, J., Fujiwara, O., Hasegawa, S., Kamataki, T., 2010. Sources and depositional processes of tsunami deposits: analysis using foraminiferal tests and hydrodynamic verification. Island Arc 19, 427–442.
Weiss, R., 2008. Sediment grains moved by passing tsunami wave: tsunami deposits in deep water. Marine Geology 250, 251–257.
Williams, H.F.L., 2009. Stratigraphy, sedimentology, and microfossil content of Hurricane Rita storm surge deposits in southwest Louisiana. Journal of Coastal Research 25, 1041–1051.
Woodroffe, S.A., Horton, B.P., Larcombe, P., Whittaker, J.E., 2005. Intertidal mangrove foraminifera from the central Great Barrier Reef shelf, Australia: implications for sea-level reconstruction. Journal of Foraminiferal Research 35, 259–270.
Yordanova, E.K., Hohenegger, J.H., 2007. Studies on settling, traction and entrainment of larger benthic foraminiferal tests: implications for accumulation in shallow marine sediments. Sedimentology 54, 1273–1306.